An intact connexin N-terminus is required for function but not gap junction formation

John W. Kyle[1], Peter J. Minogue[2], Bettina C. Thomas[2], Denise A. Lopez Domowicz[2], Viviana M. Berthoud[2], Dorothy A. Hanck[1] and Eric C. Beyer[2,*]

[1]Department of Medicine, Section of Cardiology and [2]Department of Pediatrics, Section of Hematology/Oncology, University of Chicago, Chicago, IL 60637, USA

*Author for correspondence (e-mail: ebeyer@peds.bsd.uchicago.edu)

Accepted 9 June 2008
Journal of Cell Science 121, 2744-2750 Published by The Company of Biologists 2008
doi:10.1242/jcs.032482

Summary

The cytoplasmic N-termini of connexins have been implicated in protein trafficking, oligomerization and channel gating. To elucidate the role of the N-terminus in connexin37 (CX37), we studied mutant constructs containing partial deletions of its 23 N-terminal amino acids and a construct with a complete N-terminus in which residues 2-8 were replaced with alanines. All mutants containing nine or more N-terminal amino acids form gap junction plaques in transiently transfected HeLa cells, whereas most of the longer deletions do not. Although wild-type CX37 allowed intercellular transfer of microinjected neurobiotin in HeLa cells and formed conducting hemichannels in *Xenopus* oocytes, none of the mutant constructs tested show evidence of channel function. However, in coexpression experiments, N-terminal mutants that formed gap junction plaques potently inhibit hemichannel conductance of wild-type CX37 suggesting their co-oligomerization. We conclude that as much as half the length of the connexin N-terminus can be deleted without affecting formation of gap junction plaques, but an intact N-terminus is required for hemichannel gating and intercellular communication.

Supplementary material available online at
http://jcs.biologists.org/cgi/content/full/121/16/2744/DC1

Key words: Connexin37, Gap junction, Intercellular communication

Introduction

Gap junctions are membrane specializations containing clusters of intercellular channels. Gap junction channels allow intercellular passage of ions and small molecules up to 1000 Da, including second messengers. These channels are oligomeric assemblies of members of a family of related proteins called connexins (reviewed by Beyer and Berthoud, 2008). Six connexin monomers assemble to form a connexon (hemichannel), which, in turn, forms a complete gap junction channel by docking with a connexon from an adjacent cell. The connexin polypeptide spans the membrane four times and has three cytoplasmic regions: the N-terminus (NT), a loop between the second and third transmembrane domains (CL), and the C-terminus (CT) (Fig. 1, top). Structural studies of gap junctions have revealed that each hemichannel contains a ring of 24 transmembrane helices, but these studies do not yet allow unambiguous assignment of these helices or boundaries of connexin domains including the NT (Unger et al., 1999; Oshima et al., 2007). Most topological models suggest that the NT of α-group connexins contains 23 amino acids and that of β-group connexins contains 22 amino acids [illustrated for connexin37 (CX37) in Fig. 1].

Heterologous expression of site-directed mutants and chimeric connexins in a number of isoforms have demonstrated the influence of amino acids within the NT upon channel properties, including transjunctional voltage (V_j)-dependent gating, unitary conductance, permeability and sensitivity to regulation by polyamines (Verselis et al., 1994; Oh et al., 2000; Purnick et al., 2000b; Musa et al., 2004; Tong et al., 2004; Dong et al., 2006). In at least some connexins, the NT influences the compatibility of connexin hetero-oligomerization, because Lagree and colleagues (Lagree et al., 2003) have shown that altering the identity of amino acids 11 and 12 in CX32 allows it to oligomerize with CX43. Thus, the cytoplasmic NT appears to be critical for determining many physiological properties of hemichannels and gap junction channels and cellular and/or biochemical behavior of the connexin proteins.

Disruption of the properties conferred by the NT may also explain why mutations within this region in different connexins lead to inherited diseases, including sensorineural deafness (CX26, CX30 and CX31; http://davinci.crg.es/deafness/), X-linked Charcot-Marie-Tooth disease (CX32; http://www.molgen.ua.ac.be/CMTMutations/), oculodentodigital dysplasia (CX43) (Paznekas et al., 2003) and congenital cataracts (CX50) (Chang et al., 2002; Willoughby et al., 2003). The cellular and physiological properties have not been examined for all of these disease-linked mutants; however, among those studied, some show impaired protein trafficking to the cell surface, whereas others traffic properly, but show loss or alterations of channel function (Deschenes et al., 1997; Ressot et al., 1998; Grifa et al., 1999; Matsuyama et al., 2001; D'Andrea et al., 2002; Richard et al., 2003; Rouan et al., 2003; Common et al., 2003; Essenfelder et al., 2004; Shibayama et al., 2005; Thomas et al., 2008).

The present experiments were designed to elucidate the importance of residues within the NT of CX37 for formation of gap junctional plaques and functional channels and hemichannels. These studies utilized expression systems that were similar to those we have previously used, including transfected mammalian cell lines for the cell biological and physiological characterization of gap junction channels (Reed et al., 1993; Veenstra et al., 1994; Larson et al., 1997; Larson et al., 2000) and *Xenopus* oocytes for studies of hemichannel currents (Puljung et al., 2004). The hemichannels were studied, because many properties of gap junction channels can be predicted from those of hemichannels (Ebihara et al., 1995; Srinivas et al., 2005). Moreover, there is evidence suggesting that

Journal of Cell Science

Journal of Cell Science

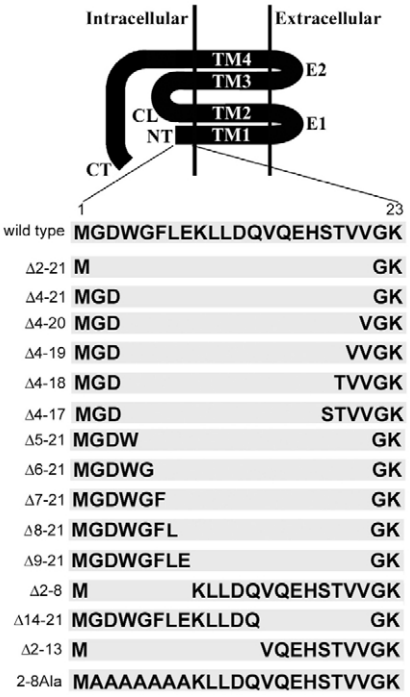

Fig. 1. Diagram showing the topology of the connexin polypeptide relative to the membrane (top) and the amino acid sequences of the N-terminal domains of wild-type CX37 and the deletion or substitution mutants (bottom). NT, amino terminal domain; CL, cytoplasmic loop; CT, C-terminal domain; TM1-TM4, transmembrane domains 1-4; E1 and E2, extracellular loops.

the behavior of CX37 hemichannels may be important in the pathogenesis of atherosclerosis (Wong et al., 2006). Gating of hemichannels to the closed conformation is also critical to prevent a large 'leak' between the cytoplasm and the extracellular space when hemichannels are transiently present in the plasma membrane after oligomerization and trafficking, but prior to docking with a partner from the apposing cell.

Results

Wild-type CX37 and many NT deletion mutants form gap junction plaques

To determine the importance of residues within the NT for formation of gap junction plaques and for function, we studied CX37 and a series of mutants in which amino acids within the NT were deleted or replaced (Fig. 1). Gap junction plaque formation was studied in HeLa cells transiently transfected with CX37 or deletion mutants. GFP was added to the C-terminus of all constructs to facilitate detection of connexins within cells and at gap junction plaques by localizing GFP fluorescence.

In HeLa cells transfected with GFP-tagged CX37, the distribution of CX37 was as expected for a wild-type gap junction protein. GFP fluorescence was very prominent at appositional membranes with large gap junction plaques frequently observed (Fig. 2A). Some of the GFP displayed a perinuclear localization, typical for membrane proteins en route to the plasma membrane (Fig. 2A). We initially studied two mutants in which most of the CX37NT was deleted (Δ2-21 and Δ4-21). We anticipated that if the NT plays a role in membrane insertion or oligomerization deleting almost all of it would lead to an altered cellular distribution. The localization of the mutant containing the longest deletion (Δ2-21) was very different from that of wild-type CX37. The Δ2-21 mutant was located exclusively in the cytoplasm where it showed a diffuse pattern; no GFP fluorescence was detected at the cell surface, and no gap junction plaques were ever observed (Fig. 2B). The mutant with the next longest deletion, Δ4-21, was localized in the cytoplasm in most cells (Fig. 2C). It was rarely found in small plaques at appositional membranes (Fig. 2D).

To determine whether a minimal length of NT was necessary for gap junction plaque formation, we studied deletion mutants in which amino acids were progressively restored to either side of the NT (Fig. 1). Among the deletion mutants containing fewer than nine

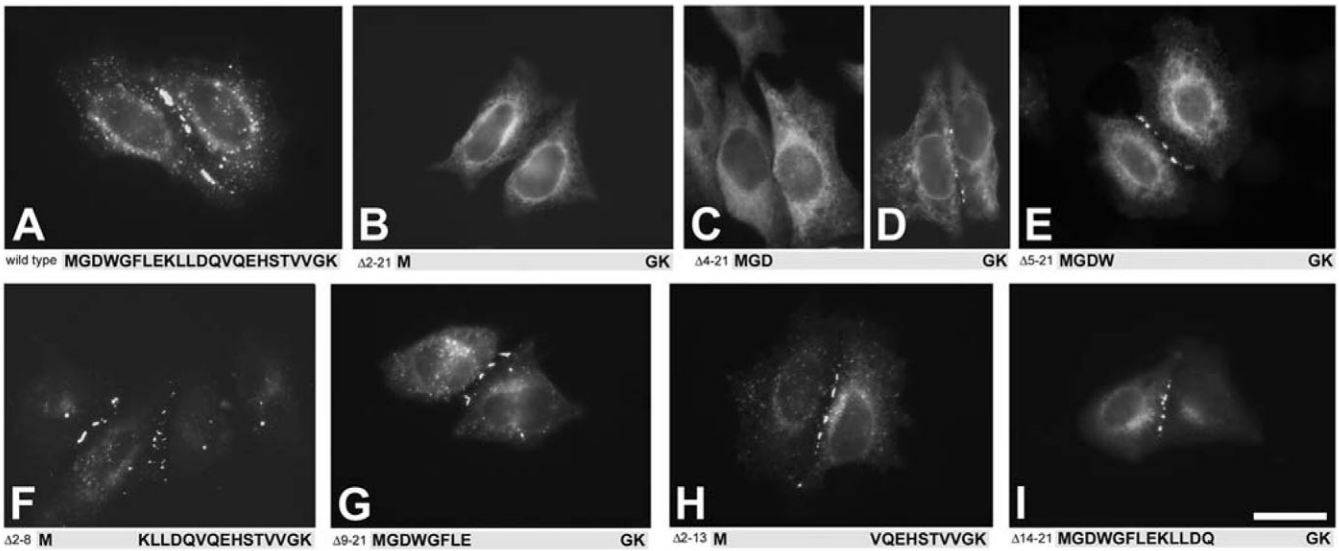

Fig. 2. Fluorescence microscopic localization of wild-type CX37 (A) and deletion mutants (B-I) after transient transfection of HeLa cells with GFP-labeled constructs. Wild-type CX37 (A), Δ5-21 (E), Δ2-8 (F), Δ9-21 (G), Δ2-13 (H) and Δ14-21 (I) each frequently showed localization to appositional membranes consistent with formation of gap junction plaques. (B) Δ2-21 was always localized in the cytoplasm, and no gap junction plaques were ever detected. Δ4-21 most commonly was found in the cytoplasm (C) and rarely between cells, in small gap junction plaques (D). Scale bar: 20 μm for A-D,G,H; 25 μm for E,F,I.

Table 1. Gap junction plaque formation in transfected HeLa cells

Construct name	Presence of gap junction plaques
Wild type	++
Δ2-21	–
Δ4-21	–/+
Δ4-20	–
Δ4-19	–
Δ4-18	–
Δ4-17	–
Δ5-21	++
Δ6-21	–
Δ7-21	–
Δ8-21	+
Δ9-21	++
Δ2-8	++
Δ14-21	++
Δ2-13	++
2-8Ala	++

++, frequent; +, less frequent; –/+, rare; –, absent.

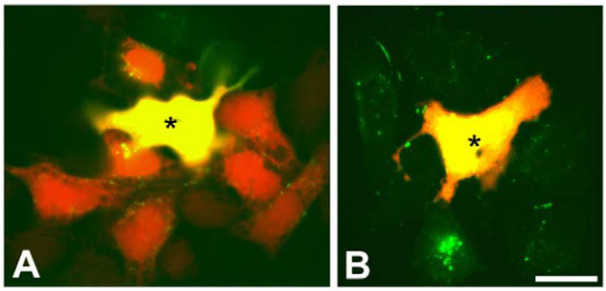

Fig. 3. Intercellular transfer of microinjected gap junction permeant tracers in transfected HeLa cells. (A, B) Photomicrographs obtained after microinjection of a solution containing Lucifer yellow (yellow) and neurobiotin (red) into HeLa cells expressing wild-type CX37 (A) or Δ2-8 (B). Neither cells expressing CX37 nor those expressing Δ2-8 showed significant intercellular transfer of Lucifer yellow beyond the injected cell (indicated by asterisk). Cells expressing wild-type CX37 displayed extensive transfer of neurobiotin, whereas those expressing Δ2-8 did not allow significant intercellular passage of this tracer. Scale bar: 30 μm.

NT amino acids, only one (Δ5-21) formed gap junction plaques of similar abundance and size to wild-type CX37 (Fig. 2E). Gap junction plaques were never observed in HeLa cells transfected with the deletion mutants Δ6-21, Δ7-21, Δ4-20, Δ4-19, Δ4-18 or Δ4-17 (Table 1, Fig. 1). The distribution of GFP fluorescence in cells expressing these constructs was similar to that of the Δ2-21 mutant (Fig. 2B). One construct containing nine NT amino acids (Δ8-21) produced some gap junction plaques, although they were less frequently observed than in cells expressing wild-type CX37 (Table 1). A deletion mutant containing 10 NT amino acids (Δ9-21) consistently formed large gap junction plaques (Fig. 2G and Table 1) similar to those seen in cells transfected with wild-type CX37.

To examine whether gap junction plaque formation required only a minimum NT length or also required specific NT amino acids, we studied two sets of mutants in which complementary stretches of 7-12 amino acids were deleted (Δ2-8 and Δ9-21; Δ2-13 and Δ14-21) (Fig. 1). Each of these mutants showed a distribution similar to wild-type CX37 and formed many intercellular plaques (Fig. 2F-I and Table 1).

Unlike wild-type CX37, NT deletion mutants did not allow intercellular transfer of gap junction tracers

The ability of CX37 and the mutant constructs to form conducting gap junction channels was tested by assaying the intercellular transfer of the low molecular mass tracers, Lucifer yellow (457 Da; charge, –2) and neurobiotin (323 Da; charge, +1). Because gap junction channels made of CX37 show limited permeability to negatively charged molecules smaller than Lucifer yellow (Veenstra et al., 1994), the inclusion of this dye in these experiments allowed identification of the injected cell, and provided a potential test of altered permeability of mutant channels compared with wild-type CX37.

Cells expressing the positive control, wild-type CX37, exhibited extensive transfer of neurobiotin, but not the negatively charged Lucifer yellow (Fig. 3A and Table 2). We initially tested Δ2-21 (a construct that did not form gap junction plaques in HeLa cells) as a negative control. As expected, cells expressing Δ2-21 did not transfer either Lucifer yellow or neurobiotin between cells at higher levels than those seen in untransfected HeLa cells (Table 2). Each of the mutants that formed gap junction plaques, Δ5-21, Δ8-21, Δ9-21, Δ2-8, Δ2-13 or Δ14-21, was tested for its ability to support intercellular transfer of neurobiotin and Lucifer yellow. Cells expressing these constructs did not show transfer of either neurobiotin or Lucifer yellow at levels higher than those seen in untransfected HeLa cells (Fig. 3B and Table 2).

NT deletion mutants did not form conducting hemichannels

We assayed for formation of conducting hemichannels in *Xenopus* oocytes injected with CX37 cRNA by two electrode voltage clamp. Control oocytes injected only with an antisense oligonucleotide to endogenous *Xenopus* CX38, when studied in extracellular zero divalent OR2 solutions without Ca^{2+} or Mg^{2+} (90 mM NaCl, 2.5 mM KCl and 5 mM HEPES, pH 7.6), showed only small currents (Fig. 4A). Extracellular solutions free of divalent cations were used because CX37 hemichannels are highly sensitive to blockage by Ca^{2+} (IC_{50} for Ca^{2+}=107 μM) and Mg^{2+} (IC_{50}=1.3 mM) (Puljung et al., 2004). Recordings from oocytes injected with CX37 cRNA showed large currents (Fig. 4B). CX37 hemichannels passed current linearly with respect to voltage over the range of –100 mV to +10 mV (Fig. 4E). CX37 hemichannel currents were almost completely blocked by the addition of 1 mM Ca^{2+} (not shown). These characteristics were essentially identical to those previously observed for wild-type CX37 without a GFP tag (Puljung et al., 2004).

Even though Δ2-21 did not form gap junction plaques or allow intercellular transfer of neurobiotin in HeLa cells, it was possible

Table 2. Neurobiotin transfer in transfected HeLa cells

Construct	Neurobiotin-filled cells (mean ± s.e.m.)	*n*
None	0.5±0.3	21
CX37	8.8±0.6*	46
Δ2-21	0.3±0.2	15
Δ5-21	0.3±0.2	16
Δ8-21	0.1±0.1	14
Δ9-21	0.2±0.1	13
Δ2-8	0.2±0.1	31
Δ2-13	0.4±0.2	16
Δ14-21	0.3±0.1	14

*P<0.001 vs. untransfected cells (None) or any of the deletion mutants. There was no significant difference between the untransfected cells (None) and any of the deletion mutants (P>0.1).

Journal of Cell Science

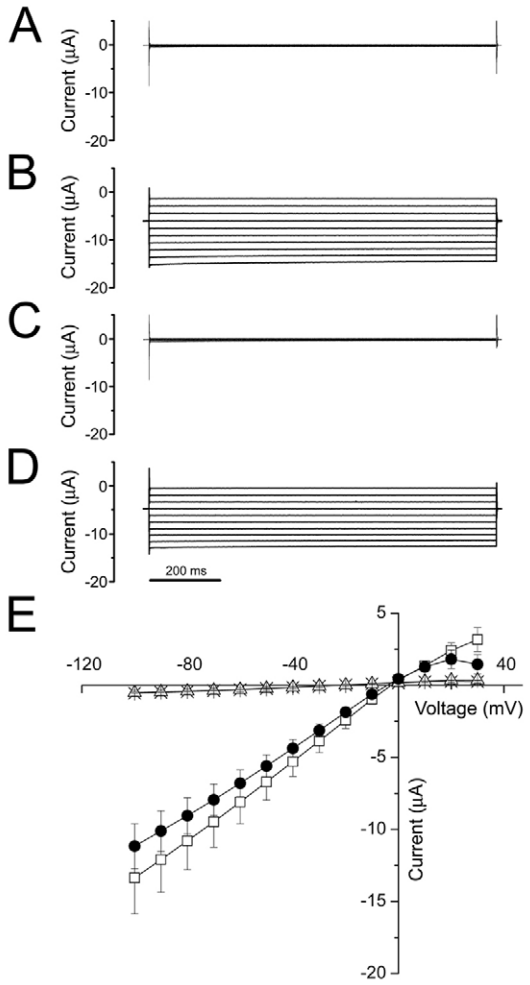

Fig. 4. Wild-type CX37 produced large hemichannel currents in *Xenopus* oocytes, but Δ2-21 did not produce currents nor inhibited wild-type currents. (A-D) Hemichannel current traces from control oocytes (A), or oocytes expressing wild-type CX37 (B), Δ2-21 (C) or wild-type CX37 and Δ2-21 (D) elicited in zero divalent OR2 by a series of voltage steps held for 1 second from a holding potential of –40 mV in 10 mV steps. Control currents shown in A were obtained from an oocyte that was injected with 2 ng antisense oligonucleotide to endogenous connexin CX38 only. Although an oocyte injected with 10 ng cRNA encoding wild-type CX37 showed hemichannel currents (B), no currents were observed above background in oocytes injected with 10 ng Δ2-21 cRNA alone (C). Oocytes injected with 10 ng wild-type CX37 cRNA and 10 ng Δ2-21 cRNA showed hemichannel currents similar in magnitude to the currents observed in oocytes injected with wild-type CX37 cRNA. (E) Current-voltage relationships obtained from control oocytes (×), or oocytes injected with wild-type CX37 (●), Δ2-21 (△), or a 1:1 mixture of Δ2-21 and CX37 (□). Data are shown as mean ± s.e.m.

that it formed a small number of conducting hemichannels at the cell surface that were below the detection limit of fluorescence microscopy. Therefore, we assayed Δ2-21 for conducting hemichannel formation in single *Xenopus* oocytes. GFP fluorescence in oocytes confirmed production of protein from the Δ2-21 construct. The pattern of fluorescence in oocytes injected with the Δ2-21 cRNA was noticeably different from that in oocytes injected with wild-type CX37 cRNA, suggesting that this protein did not reach the oocyte surface (data not shown). Oocytes injected with cRNA encoding Δ2-21 did not show connexin hemichannel currents above background levels determined in control oocytes (Fig. 4C), consistent with the observation that Δ2-21 protein probably did not traffic to the oocyte surface. To test whether Δ2-21 could coassemble with wild-type CX37 and alter wild-type function, these constructs were co-expressed in *Xenopus* oocytes. Co-expression of Δ2-21 had no effect upon wild-type CX37 currents (Fig. 4D,E). We conclude that Δ2-21 does not form conducting hemichannels and does not participate in connexon formation with wild-type CX37. Based on these results, we did not further study function in deletion mutants that did not form gap junction plaques.

Although no gap junction channel function was detected in any of the deletion mutants tested for transfer of neurobiotin, it remained possible that these constructs might form channels with reduced permeability that could still conduct current-carrying ions. We chose several of the plaque-forming deletion mutants (Δ2-8, Δ9-21, Δ2-13 and Δ14-21) for further study of connexin hemichannel function. Oocytes injected with each of these GFP-tagged constructs were very green 2 days after injection, and GFP could be seen at or near the oocyte surface. Currents recorded from single GFP-positive oocytes injected with the corresponding cRNAs were not significantly larger than those observed in control oocytes (Fig. 5A,B and data not shown), indicating that none of these constructs formed conducting connexin hemichannels.

Even though these deletion mutants did not form conducting hemichannels, it was possible that they might co-oligomerize with wild-type CX37 and affect function. We tested the ability of the two complementary constructs (Δ2-8 and Δ9-21) to co-assemble with wild-type CX37 by co-injection of their cRNAs with wild-type CX37 cRNA in *Xenopus* oocytes. Both Δ2-8 and Δ9-21 were potent inhibitors of wild-type CX37 currents (Fig. 5A and B). Dominant-negative behavior would be expected if Δ2-8 and Δ9-21 co-assembled with wild-type CX37 and formed non-conducting hemichannels. The degree of inhibition can indicate the number of mutant subunits required to poison the hemichannel. To examine the potency of inhibition, different ratios of mutant to wild-type cRNAs were injected into *Xenopus* oocytes. Data suggested that for either Δ2-8 or Δ9-21, inclusion of one mutant connexin per hemichannel was sufficient to inhibit hemichannel function (Fig. 5C and D).

Maintaining the length of the NT by substituting alanines for deleted residues 2-8 did not rescue function

It was possible that the lack of functional hemichannels produced by NT deletion constructs that reached the cell surface and formed plaques was due to the requirement for a specific length of the NT regardless of amino acid sequence. Therefore, we prepared a construct (2-8Ala) in which residues 2-8 were replaced with alanines (in an attempt to 'repair' Δ2-8). Fluorescence microscopy showed that 2-8Ala formed gap junction plaques after transfection of HeLa cells (Fig. 6A). No significant intercellular transfer of neurobiotin was observed after microinjection into 2-8Ala transfected HeLa cells. (Neurobiotin was detected in 0.3±0.1 neighbors, n=12 injections.) When expressed in *Xenopus* oocytes, 2-8Ala did not produce hemichannels that displayed voltage-dependent currents, but it did strongly inhibit currents from coexpressed wild-type CX37 at a 1:1 ratio (Fig. 6B). These results suggest that at least some of the amino acid residues in positions 2-8 are essential for hemichannel currents.

Discussion

We used mutants with partial deletions of the 23 amino acid CX37 NT to define the importance of specific regions of the NT in

Journal of Cell Science

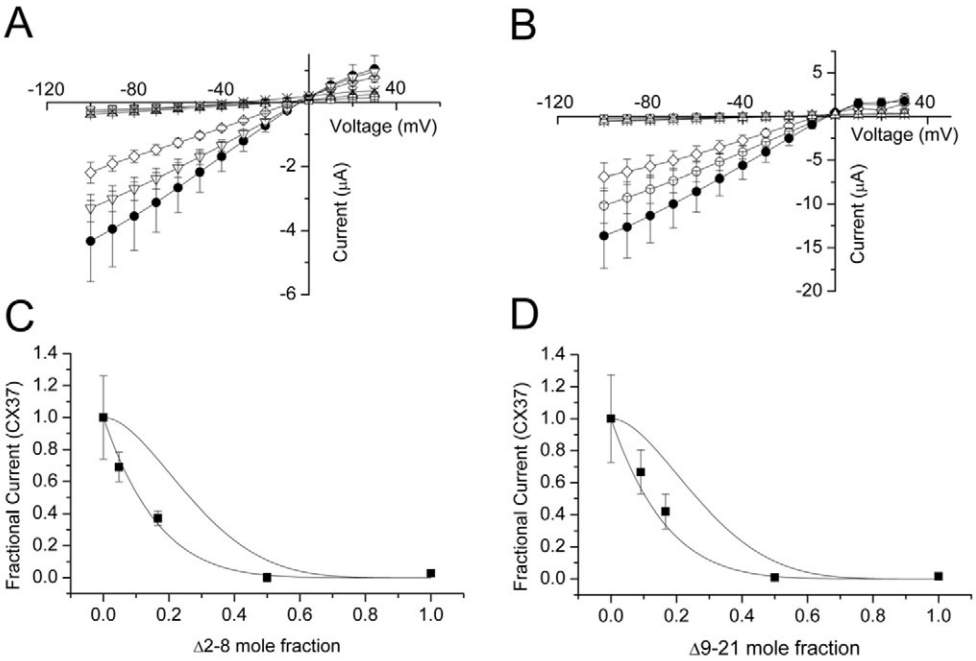

Fig. 5. Mutants Δ2-8 and Δ9-21 did not produce conducting hemichannels, but coexpression of either one with wild-type CX37 inhibited currents produced from wild-type CX37. (A) Current-voltage relationships for control oocytes (×), wild-type CX37 (●), Δ2-8 (△) and differing ratios of Δ2-8 coexpressed with wild-type CX37 (□, 1:1; ◇, 0.2:1; ▽, 0.05:1). (B) Current-voltage relationships for wild-type CX37 (●), Δ9-21 (△), and differing ratios of Δ9-21 coexpressed with wild-type CX37 (□, 1:1; ◇, 0.2:1; ○, 0.1:1). (C,D) Graphs of mole fraction vs fractional current for Δ2-8 coexpressed with wild-type CX37 (C) and for Δ9-21 coexpressed with wild-type CX37 (D). Curves represent the theoretical values for inhibition by one (lower) or two (upper) mutant subunits within a hemichannel. Both Δ2-8 and Δ9-21 fit closely to the curve for inhibition of hemichannel function by one mutant subunit. Data are shown as mean ± s.e.m.

formation of gap junction plaques, formation of functional conducting hemichannels and establishment of intercellular communication.

All constructs that contained more than nine NT amino acids formed plaques, even though different regions of the NT had been deleted (Table 1). Since oligomerization and trafficking to the plasma membrane must occur before plaque formation, it is likely that these processes were also normal in these mutants. The mutants that did not form plaques were primarily the larger deletions. These results suggest that a minimal length of NT is required for proper insertion of transmembrane regions or oligomerization and targeting to the plasma membrane and formation of gap junction plaques. Although this simple interpretation is appealing, there were two notable exceptions to this trend. Both Δ4-21 (rarely) and Δ5-21 (as frequently as wild-type CX37) formed plaques even though they contained only 5 or 6 NT amino acids, so there must be other features that can overcome the requirement for a minimal length. The only difference between these two constructs is the presence of a tryptophan (W4) in Δ5-21, which suggested the possible importance of this residue for plaque formation. However, two other deletion mutants (Δ2-8 and Δ2-13) readily formed plaques despite the absence of this residue. Moreover, gap junction plaques were also observed in HeLa cells transfected with a CX37 mutant containing a substitution of an alanine for this tryptophan (CX37W4A) (data not shown).

Four different deletion mutants in which complementary stretches of NT amino acids were deleted (Δ2-8 and Δ9-21; Δ2-13 and Δ14-21) readily formed gap junction plaques. These deletions cover almost all of the amino acids in the NT and show that amino acids from either end of the NT between 2 and 21 can be deleted without affecting gap junction plaque formation. Moreover, each of the amino acids between 2 and 21 was deleted in some constructs that still formed gap junction plaques. Thus, the critical features or tertiary structure required for plaque formation are found in more than one region of the NT.

Despite the formation of plaques by many of our deletion and substitution mutants, none of them formed functional channels as detected by hemichannel currents in *Xenopus* oocytes or by neurobiotin transfer in transfected HeLa cells. This is not an entirely surprising result, because some of the disease-associated mutants that have been studied form plaques, but not functional channels (Deschenes et al., 1997). However, many point mutants of the

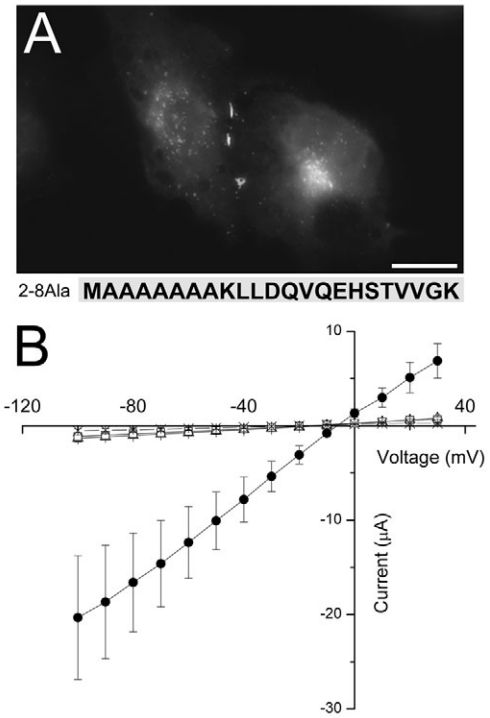

Fig. 6. A mutant containing alanine residues substituted for the amino acids at positions 2-8 formed plaques in transfected HeLa cells, did not form functional hemichannels but inhibited wild-type CX37 function. (A) Fluorescence microscopic localization of 2-8Ala in HeLa cells after transient transfection. Scale bar: 20 μm. (B) Current-voltage relationships for control oocytes (×), wild-type CX37 (●), 2-8Ala (△) and 2-8Ala coexpressed with wild-type CX37 at a 1:1 ratio (□). Data are shown as mean ± s.e.m.

Journal of Cell Science

connexin NT yield functional channels, albeit with altered channel properties (Verselis et al., 1994; Purnick et al., 2000b; Musa et al., 2004; Dong et al., 2006; Tong and Ebihara, 2006). Taken together, our results demonstrate that plaque formation by a connexin variant does not ensure gap junction function and that the NT is critical for formation of conducting hemichannels. Moreover, channel function requires more than an intact length of the NT as shown by the failure of the alanine substitution mutant (2-8Ala) to restore function. The failure of multiple complementary deletion mutants to form conducting hemichannels or gap junction channels implies that there are multiple residues among amino acids 2-21 that are required for channel function.

Purnick and colleagues (Purnick et al., 2000a) proposed a model for the NT of CX26 based on determination of the structure of a 15 amino acid peptide by nuclear magnetic resonance spectroscopy. Their model has an α-helix extending from position 1 to 10 and a critical bend at positions 11 and 12 (corresponding to amino acids 12 and 13 in CX37) which was suggested to act as a 'hinge' allowing the first 10 amino acids to swing into (and block) the channel. Recently, Oshima and co-workers (Oshima et al., 2007) presented structural studies of a 'permeability' mutant of CX26 (Oshima et al., 2003). Their studies showed a density within the pore of the channel, which they suggested might represent a bundle of N-termini acting as a 'plug' to close the channel. If the 'plug gating' inferred from these studies applied to CX37, we might have anticipated that removal of the 'plug' in our deletion mutants might have removed all gating and yielded channels that conducted large currents (rather than none) or a hemichannel that could not close. Rather, our data can be interpreted as suggesting a requirement of an intact NT to hold the channel open (instead of acting as a gating plug), and when the NT is altered or removed, the channel closes. Thus, it is possible that the NT of the CX26 mutant studied by Oshima et al. (Oshima et al., 2007) has lost this ability and associates (or bundles) with nearby NTs leading to the observation of a 'plug', a hypothesis that will require further investigation. Alternatively, it is possible that the N-termini of CX26 and CX37 (being members of different connexin subfamilies α and β) have different structures and their channels are gated by different mechanisms. Moreover, if the 'plug' model applied to CX37, the α-helix structure of the Purnick model should have been preserved in the 2-8Ala substitution mutant; however, this mutant was not functional. These results suggest that one or more residues in positions 2-8 are important interaction sites for hemichannel and complete channel gating.

Several mutants (Δ2-8, Δ9-21 and 2-8Ala) acted as potent inhibitors when coexpressed with wild-type CX37. Indeed, for the two that we studied in detail, Δ2-8 and Δ9-21, only one mutant subunit out of six subunits was sufficient to poison function (conducting hemichannels). The simplest explanation for this dominant-negative behavior is that hetero-oligomerization of the nonfunctional subunit with wild-type subunits resulted in a nongating hemichannel.

Many types of gating have been described for connexin hemichannels (including voltage-dependent gating and 'loop' gating) (Trexler et al., 1996) implying that there are at least two distinct gates localized in different regions of the connexin molecule. Some features that affect gating (like the voltage sensor) may reside in the NT (Purnick et al., 2000b). But, the NT does not need to be the gate itself. Loss of conductance in the NT deletion mutants might also result if an intact NT is required for the other gates to be operative. Moreover, the coexpression experiments showing the dominant-negative behavior of Δ2-8 and Δ9-21 implies that all six N-termini must be intact for proper gating.

Taken together, our observations suggest that many of the NT residues are not required for membrane insertion, oligomerization, trafficking to the plasma membrane and formation of gap junction plaques. However, the NT serves an essential role in hemichannel and gap junction channel gating.

Materials and Methods

Chemicals

All chemicals were obtained from Sigma Chemical Co. (St Louis, MO) unless otherwise specified.

Generation of GFP-tagged wild-type CX37 and NT deletion mutants

The coding region of CX37 was PCR amplified with CX37 antisense and sense primers (supplementary material Table S1) using human CX37 DNA encoding a serine at position 319 as template and the TaKaRa LA Taq polymerase (Takara Bio USA, Madison, WI). A C-terminal GFP tag was produced by amplification of the Emerald variant (Invitrogen, Carlsbad, CA) of green fluorescent protein (GFP) using sense and anti-sense primers (supplementary material Table S1) and Phusion High-Fidelity DNA Polymerase (New England Biolabs, Ipswich, MA). The primers introduced a *Sna*BI restriction site at the end of the coding region of CX37 and at the beginning of the coding region of GFP. The PCR products were subcloned into pGEMTEasy (Promega, Madison, WI) and fully sequenced. The construct for the wild-type CX37-GFP fusion protein was obtained by ligating the *Sna*BI-*Sac*I GFP insert into the CX37pGEMTEasy construct linearized with *Sna*BI and *Sac*I.

CX37-GFP was subcloned into the *Eco*RI site of pBSSK-XG (containing the 5′ and 3′ untranslated regions of the *Xenopus* globin gene bracketing an *Eco*RI site and inserted between the *Hin*dIII and *Pst*I sites of pBSSK with the *Eco*RI site in the polylinker removed (Stratagene, La Jolla, CA) for oocyte expression (Satin et al., 1992) and, after blunting the *Eco*RI ends, into the *Eco*RV site of pcDNA3.1/Hygro(+) (Invitrogen, Carlsbad, CA) for expression in mammalian cells. All deletion mutants were obtained by PCR using the Phusion High-Fidelity DNA polymerase, CX37GFP in pGEMTEasy, pcDNA3.1/Hygro(+) or pBSSK-XG as the template and the sets of primers indicated in supplementary material Table S1. The deletion mutants obtained in pGEMTEasy were subsequently subcloned in the two expression plasmids as described for wild-type CX37. The primers were selected to amplify the entire constructs except the nucleotides that encoded the deleted NT amino acids.

CX37GFP in pBSSK-XG was used as template to obtain the 2-8Ala substitution mutant using the set of primers indicated in supplementary material Table S1. To obtain the 2-8Ala substitution mutant in a mammalian expression vector, the *Eco*RI insert was subcloned into the *Eco*RI site of pcDNA3.1(+) (Invitrogen).

The coding region of all constructs was fully sequenced at the Cancer Research Center DNA Sequencing Facility of the University of Chicago to ensure that PCR amplification did not introduce additional unwanted mutations. This series of constructs encoded CX37 with different deletions from the CX37NT and an alanine substitution (Fig. 1).

Cell culture and transfections

All cell culture media and supplements were obtained from Invitrogen unless otherwise noted. HeLa cells were grown in MEM supplemented with 0.1 mM nonessential amino acids, 10% fetal bovine serum (US Bio-Technologies, Pottstown, PA), 2 mM glutamine, 10 U/ml penicillin G and 10 μg/ml streptomycin sulfate. Transfections were carried out using Lipofectin and PLUS Reagent following the manufacturer's instructions.

Fluorescence microscopy

Transfected cells cultured on four-well chamber slides (LAB TEK, Nalge Nunc International, Naperville, IL) or glass coverslips were fixed with 4% paraformaldehyde in phosphate-buffered saline (PBS) pH 7.4 for 30 minutes at room temperature. After rinsing cells with PBS, coverslips were mounted using 2% n-propylgallate in PBS/glycerol (1:1).

Specimens were studied with a Zeiss Plan Apochromat 40× objective in an Axioplan 2 microscope (Carl Zeiss, München, Germany). Images were captured with an Axiocam digital camera (Carl Zeiss) using Zeiss AxioVision software.

Microinjection of gap junction tracers

Cells cultured on glass coverslips (80-90% confluency) were transferred to F-12 medium (Invitrogen) buffered with 15 mM HEPES, pH 7.4. Clusters of connexin-expressing cells were identified based on their GFP fluorescence. Individual cells were impaled and injected with a solution containing 5% Lucifer yellow (Molecular Probes) and 4% neurobiotin (Vector Laboratories, Burlingame, CA) in water for 3 minutes using a picospritzer (model PLI-188, Nikon Instruments, Melville, NY).

After injection, cells were fixed in 4% paraformaldehyde for 30 minutes and then permeabilized with methanol/acetone (1:1) for 2 minutes at room temperature. The neurobiotin tracer was detected by staining the cells with Cy3-streptavidin conjugate (Sigma) for 30 minutes at room temperature. The extent of intercellular transfer of

both tracers was determined by counting the number of adjacent cells containing the tracer. Statistical analysis was performed using Student's *t*-test.

RNA and oocyte preparation

The CX37 DNA templates were linearized with *Xba*I and transcribed using the T7 mMessage mMachine Kit (Applied Biosystems/Ambion, Austin, TX). Stage V and VI oocytes were harvested from adult female *Xenopus laevis* under tricaine anesthesia, treated with collagenase (2 mg/ml for 90 minutes) in 0 Ca^{2+}OR2 (90 mM NaCl, 2.5 mM KCl, 1 mM $MgCl_2$ and 5 mM HEPES, pH 7.6), and manually defolliculated in $OR2^+$ (90 mM NaCl, 2.5 mM KCl, 1 mM $MgCl_2$, 1 mM $CaCl_2$, 0.27 g/l sodium pyruvate, 2 mg/l gentamicin, 50 U/ml penicillin, 50 μg/ml streptomycin and 5 mM HEPES, pH 7.6). Oocytes were injected with 10-50 ng cRNA in a total volume of 50 nl. Antisense oligonucleotide directed against the endogenous *Xenopus* CX38 protein (1 ng/μl) was included to inhibit endogenous connexin expression (Barrio et al., 1991). Injected oocytes were incubated in zero divalent OR2 (90 mM NaCl, 2.5 mM KCl and 5 mM HEPES, pH 7.6) before recording to relieve extracellular divalent block of CX37 hemichannels.

Oocyte electrophysiology

Electrophysiological recordings from oocytes were performed using two-microelectrode voltage clamp in 0 Ca^{2+}OR2 unless otherwise indicated. Pipettes were pulled to a resistance of 0.3-1.0 MΩ and filled with 3 M KCl. Recordings were performed using a Dagan CA1 oocyte clamp (Dagan Corporation, Minneapolis, MN). Signals were digitized with a Digidata 1600 analogue/digital converter (Axon Instruments, Sunnyvale, CA) at 1 kHz using pClamp 8 (Axon Instruments). All experiments were performed at room temperature (20-24°C). Data analysis was performed using MATLAB version 6.5 (The Math Works, Natick, MA) and Microcal Origin version 7.5 (OriginLab, Northampton, MA). Group statistics are reported as mean ± s.e.m.

To obtain an estimate of the number of mutant channels required to inhibit hemichannel currents, we followed the approach of Pal et al. (Pal et al., 1999) but modified the distribution equation to reflect the six subunits in a hemichannel. The function used to model the theoretical inhibition of current through a hexamer where one subunit is sufficient to inhibit current is: $y=(1-x)^6$, where x represents the mole fraction of mutant to wild-type connexin. For two mutant subunits the function becomes: $y=(1-x)^6 + 6\times(1-x)^5$. In the experiments shown, the total amount of wild-type CX37 cRNA was held constant in each mixture while mutant cRNA was varied. This analysis assumes that the translation efficiencies are the same for mutant and wild-type connexins, oligomerization of connexins into hemichannels is random and unaltered by mutant channels and hemichannel turnover rates on the cell surface are similar.

This work was supported by a fellowship within the Postdoc Program of the German Academic Exchange Service (to B.C.T.) and NIH Grant HL59199 (to E.C.B.). The authors greatly appreciate the contribution of Jonathan Budzig during the early phases of this project.

References

Barrio, L. C., Suchyna, T., Bargiello, T., Xu, L. X., Roginski, R. S., Bennett, M. V. L. and Nicholson, B. J. (1991). Gap junctions formed by connexins 26 and 32 alone and in combination are differently affected by applied voltage. *Proc. Natl. Acad. Sci. USA* **88**, 8410-8414.

Beyer, E. C. and Berthoud, V. M. (2008). The family of connexin genes. In *Connexin Biology* (ed. A. L. Harris and D. Locke) (in press).

Chang, B., Wang, X., Hawes, N. L., Ojakian, R., Davisson, M. T., Lo, W. K. and Gong, X. H. (2002). A *Gja8* (Cx50) point mutation causes an alteration of α3 connexin (Cx46) in semi-dominant cataracts of *Lop10* mice. *Hum. Mol. Genet.* **11**, 507-513.

Common, J. E., Di W. L., Davies, D., Galvin, H., Leigh, I. M., O'Toole, E. A. and Kelsell, D. P. (2003). Cellular mechanisms of mutant connexins in skin disease and hearing loss. *Cell Commun. Adhes.* **10**, 347-351.

D'Andrea, P., Veronesi, V., Bicego, M., Melchionda, S., Zelante, L., Di Iorio, E., Bruzzone, R. and Gasparini, P. (2002). Hearing loss: frequency and functional studies of the most common connexin26 alleles. *Biochem. Biophys. Res. Commun.* **296**, 685-691.

Deschenes, S. M., Walcott, J. L., Wexler, T. L., Scherer, S. S. and Fischbeck, K. H. (1997). Altered trafficking of mutant connexin32. *J. Neurosci.* **17**, 9077-9084.

Dong, L., Liu, X., Li, H., Vertel, B. M. and Ebihara, L. (2006). Role of the N-terminus in permeability of chicken connexin45.6 gap junctional channels. *J. Physiol.* **576**, 787-799.

Ebihara, L., Berthoud, V. M. and Beyer, E. C. (1995). Distinct behavior of connexin56 and connexin46 gap junctional channels can be predicted from the behavior of their hemi-gap-junctional channels. *Biophys. J.* **68**, 1796-1803.

Essenfelder, G. M., Bruzzone, R., Lamartine, J., Charollais, A., Blanchet-Bardon, C., Barbe, M. T., Meda, P. and Waksman, G. (2004). Connexin30 mutations responsible for hidrotic ectodermal dysplasia cause abnormal hemichannel activity. *Hum. Mol. Genet.* **13**, 1703-1714.

Grifa, A., Wagner, C. A., D'Ambrosio, L., Melchionda, S., Bernardi, F., Lopez-Bigas, N., Rabionet, R., Arbones, M., Monica, M. D., Estivill, X. et al. (1999). Mutations in *GJB6* cause nonsyndromic autosomal dominant deafness at *DFNA3* locus. *Nat. Genet.* **23**, 16-18.

Lagree, V., Brunschwig, K., Lopez, P., Gilula, N. B., Richard, G. and Falk, M. M. (2003). Specific amino-acid residues in the N-terminus and TM3 implicated in channel function and oligomerization compatibility of connexin43. *J. Cell Sci.* **116**, 3189-3201.

Larson, D. M., Wrobleski, M. J., Sagar, G. D. V., Westphale, E. M. and Beyer, E. C. (1997). Differential regulation of connexin43 and connexin37 in endothelial cells by cell density, growth, and TGF-β1. *Am. J. Physiol., Cell Physiol.* 272, C405-C415.

Larson, D. M., Seul, K. H., Berthoud, V. M., Lau, A. F., Sagar, G. D. V. and Beyer, E. C. (2000). Functional expression and biochemical characterization of an epitope-tagged connexin37. *Mol. Cell. Biol. Res. Commun.* **3**, 115-121.

Matsuyama, W., Nakagawa, M., Moritoyo, T., Takashima, H., Umehara, F., Hirata, K., Suehara, M. and Osame, M. (2001). Phenotypes of X-linked Charcot-Marie-Tooth disease and altered trafficking of mutant connexin 32 (*GJB1*). *J. Hum. Genet.* **46**, 307-313.

Musa, H., Fenn, E., Crye, M., Gemel, J., Beyer, E. C. and Veenstra, R. D. (2004). Amino terminal glutamate residues confer spermine sensitivity and affect voltage gating and channel conductance of rat connexin40 gap junctions. *J. Physiol.* **557**, 863-878.

Oh, S., Abrams, C. K., Verselis, V. K. and Bargiello, T. A. (2000). Stoichiometry of transjunctional voltage-gating polarity reversal by a negative charge substitution in the amino terminus of a connexin32 chimera. *J. Gen. Physiol.* **116**, 13-32.

Oshima, A., Doi, T., Mitsuoka, K., Maeda, S. and Fujiyoshi, Y. (2003). Roles of Met-34, Cys-64, and Arg-75 in the assembly of human connexin 26: Implication for key amino acid residues for channel formation and function. *J. Biol. Chem.* **278**, 1807-1816.

Oshima, A., Tani, K., Hiroaki, Y., Fujiyoshi, Y. and Sosinsky, G. E. (2007). Three-dimensional structure of a human connexin26 gap junction channel reveals a plug in the vestibule. *Proc. Natl. Acad. Sci. USA* **104**, 10034-10039.

Pal, J. D., Berthoud, V. M., Beyer, E. C., Mackay, D., Shiels, A. and Ebihara, L. (1999). Molecular mechanism underlying a Cx50-linked congenital cataract. *Am. J. Physiol* 276, C1443-C1446.

Paznekas, W. A., Boyadjiev, S. A., Shapiro, R. E., Daniels, O., Wollnik, B., Keegan, C. E., Innis, J. W., Dinulos, M. B., Christian, C., Hannibal, M. C. et al. (2003). Connexin 43 (*GJA1*) mutations cause the pleiotropic phenotype of oculodentodigital dysplasia. *Am. J. Hum. Genet.* **72**, 408-418.

Puljung, M. C., Berthoud, V. M., Beyer, E. C. and Hanck, D. A. (2004). Polyvalent cations constitute the voltage gating particle in human connexin37 hemichannels. *J. Gen. Physiol.* **124**, 587-603.

Purnick, P. E., Benjamin, D. C., Verselis, V. K., Bargiello, T. A. and Dowd, T. L. (2000a). Structure of the amino terminus of a gap junction protein. *Arch. Biochem. Biophys.* **381**, 181-190.

Purnick, P. E., Oh, S., Abrams, C. K., Verselis, V. K. and Bargiello, T. A. (2000b). Reversal of the gating polarity of gap junctions by negative charge substitutions in the N-terminus of connexin 32. *Biophys. J.* **79**, 2403-2415.

Reed, K. E., Westphale, E. M., Larson, D. M., Wang, H. Z., Veenstra, R. D. and Beyer, E. C. (1993). Molecular cloning and functional expression of human connexin37, an endothelial cell gap junction protein. *J. Clin. Invest.* **91**, 997-1004.

Ressot, C., Gomes, D., Dautigny, A., Pham-Dinh, D. and Bruzzone, R. (1998). Connexin32 mutations associated with X-linked Charcot-Marie-Tooth disease show two distinct behaviors: loss of function and altered gating properties. *J. Neurosci.* **18**, 4063-4075.

Richard, G., Brown, N., Rouan, F., Van der Schroeff, J. G., Bijlsma, E., Eichenfield, L. E., Sybert, V. P., Greer, K. E., Hogan, P., Campanelli, C. et al. (2003). Genetic heterogeneity in erythrokeratodermia variabilis: Novel mutations in the connexin gene *GJB4* (Cx30.3) and genotype-phenotype correlations. *J. Invest. Dermatol.* **120**, 601-609.

Rouan, F., Lo, C. W., Fertala, A., Wahl, M., Jost, M., Rodeck, U., Uitto, J. and Richard, G. (2003). Divergent effects of two sequence variants of *GJB3* (G12D and R32W) on the function of connexin 31 in vitro. *Exp. Dermatol.* **12**, 191-197.

Satin, J., Kyle, J. W., Chen, M., Rogart, R. B. and Fozzard, H. A. (1992). The cloned cardiac Na channel alpha-subunit expressed in *Xenopus* oocytes show gating and blocking properties of native channels. *J. Membr. Biol.* **130**, 11-22.

Shibayama, J., Paznekas, W., Seki, A., Taffet, S., Jabs, E. W., Delmar, M. and Musa, H. (2005). Functional characterization of connexin43 mutations found in patients with oculodentodigital dysplasia. *Circ. Res.* **96**, e83-e91.

Srinivas, M., Kronengold, J., Bukauskas, F. F., Bargiello, T. A. and Verselis, V. K. (2005). Correlative studies of gating in Cx46 and Cx50 hemichannels and gap junction channels. *Biophys. J.* **88**, 1725-1739.

Thomas, B. C., Minogue, P. J., Valiunas, V., Kanaporis, G., Brink, P. R., Berthoud, V. M. and Beyer, E. C. (2008). Cataracts are caused by alterations of a critical N-terminal positive charge in connexin50. *Invest. Ophthalmol. Vis. Sci.* **49**, 2549-2556.

Tong, J. J. and Ebihara, L. (2006). Structural determinants for the differences in voltage gating of chicken Cx56 and Cx45.6 gap-junctional hemichannels. *Biophys. J.* **91**, 2142-2154.

Tong, J. J., Liu, X., Dong, L. and Ebihara, L. (2004). Exchange of gating properties between rat cx46 and chicken cx45.6. *Biophys. J.* **87**, 2397-2406.

Trexler, E. B., Bennett, M. V. L., Bargiello, T. A. and Verselis, V. K. (1996). Voltage gating and permeation in a gap junction hemichannel. *Proc. Natl. Acad. Sci. USA* **93**, 5836-5841.

Unger, V. M., Kumar, N. M., Gilula, N. B. and Yeager, M. (1999). Three-dimensional structure of a recombinant gap junction membrane channel. *Science* **283**, 1176-1180.

Veenstra, R. D., Wang, H. Z., Beyer, E. C., Ramanan, S. V. and Brink, P. R. (1994). Connexin37 forms high conductance gap junction channels with subconductance state activity and selective dye and ionic permeabilities. *Biophys. J.* **66**, 1915-1928.

Verselis, V. K., Ginter, C. S. and Bargiello, T. A. (1994). Opposite voltage gating polarities of two closely related connexins. *Nature* **368**, 348-351.

Willoughby, C. E., Arab, S., Gandhi, R., Zeinali, S., Arab, S., Luk, D., Billingsley, G., Munier, F. L. and Heon, E. (2003). A novel *GJA8* mutation in an Iranian family with progressive autosomal dominant congenital nuclear cataract. *J. Med. Genet.* 40, e124.

Wong, C. W., Christen, T., Roth, I., Chadjichristos, C. E., Derouette, J. P., Foglia, B. F., Chanson, M., Goodenough, D. A. and Kwak, B. R. (2006). Connexin37 protects against atherosclerosis by regulating monocyte adhesion. *Nat. Med.* **12**, 950-954.

Table S1. List of Primers

Construct	Set of primers
Wild type CX37	CX37s: 5′-CCGGGAGCCATGGGTGACTGGGGCTTCCTG-3′ CX37as: 5′-GGC**TACGTA**CTGCTTCTTAGAAGCAGAGCTGCTGGGACGACTTGGG-3′ EMDs: 5′-CAG**TACGTA**GGTATGGTGAGCAAGGGCGAGGAGCTG-3′ EMDas: 5′-CGCTTACTTGTACAGCTCGTCCATGCCGAGAGT-3′
Δ2-21	s: 5′-GGTAAGATCTGGCTGACGGTGCTCTTC-3′ as: 5′- CATGGCTCCCGGAATCGAATTCCCGC-3′
Δ4-21	s: 5′-GGTAAGATCTGGCTGACGGTGCTCTTC-3′ as: 5′-GTCACCCATGGCTCCCGGAATCGAATT-3′
Δ4-20	s: 5′-GTGGGTAAGATCTGGCTGACGGTGCTCTTC-3′ as: 5′-GTCACCCATGGCTCCCGGAATCGAATT-3′
Δ4-19	s: 5′-GTGGTGGGTAAGATCTGGCTGACGGTGCTC-3′ as: 5′-GTCACCCATGGCTCCCGGAATCGAATT-3′
Δ4-18	s: 5′-ACCGTGGTGGGTAAGATCTGGCTGACGGT-3′ as: 5′-GTCACCCATGGCTCCCGGAATCGAATT-3′
Δ4-17	s: 5′-TCGACCGTGGTGGGTAAGATCTGGCTGAC-3′ as: 5′-GTCACCCATGGCTCCCGGAATCGAATT-3′
Δ5-21	s: 5′-GGTAAGATCTGGCTGACGGTGCTCTTC-3′ as: 5′-CCAGTCACCCATGGCTCCCGGAATCGAATT-3′
Δ6-21	s: 5′-GGTAAGATCTGGCTGACGGTGCTCTTC-3′ as: 5′-GCCCCAGTCACCCATGGCTCCCGGAAT-3′
Δ7-21	s: 5′-GGTAAGATCTGGCTGACGGTGCTCTTC-3′ as: 5′-GAAGCCCCAGTCACCCATGGCTCCCG-3′
Δ8-21	s: 5′-GGTAAGATCTGGCTGACGGTGCTCTTC-3′ as: 5′-CAGGAAGCCCCAGTCACCCATGGCTCC-3′
Δ9-21	s: 5′-GGTAAGATCTGGCTGACGGTGCTCTTC-3′ as: 5′-CTCCAGGAAGCCCCAGTCACCCATGG-3′’
Δ2-8	s: 5′-AAGTTGCTGGACCAGGTCCAGGAGCAC-3′ as: 5′-CATGGCTCCCGGAATCGAATTCCCGC-3′
Δ14-21	s: 5′-GGTAAGATCTGGCTGACGGTGCTCTTC-3′ as: 5′-CTGGTCCAGCAACTTCTCCAGGAAGC-3′
Δ2-13	s: 5′-GTCCAGGAGCACTCGACCGTGGTGGGT-3′ as: 5′-CATGGCTCCCGGAATCGAATTCCCGC-3′